

DETECTION OF EMBOLIC SIGNALS USING WAVELET TRANSFORM

N. Aydin, H.S. Markus

Department of Clinical Neurosciences
Guy's, King's and St Thomas' School of Medicine and Institute of Psychiatry
De Crespigny Park, Denmark Hill, London SE5 8AF, UK
E-mail: nizamettin.aydin@kcl.ac.uk

ABSTRACT

Early and accurate detection of microemboli is important for monitoring of preventive therapy in stroke-prone patients. Embolic signals have large amplitude and show transient characteristics because of their reflectivity and size compared to the blood cells. One of the problems in detection of microemboli is the identification of an embolic signal caused by very small microemboli. The amplitude of the embolic signal may be so small as to require some sort of advanced processing techniques to distinguish these signals from Doppler signals arising from red blood cells. The windowed Fourier transform (WFT) has been widely used by commercial Doppler ultrasonic systems. However it is not ideally suited to analysis of short duration embolic signals due to an inherent trade-off between time and frequency resolution. An alternative approach is the wavelet transform, which might be expected to describe embolic signals well. In this paper we show that the temporal resolution and time localisation of the wavelet transform are better than that of the WFT.

1. INTRODUCTION

Doppler ultrasound can be used to detect circulating cerebral emboli [1]. Emboli passing through the sample volume result in a short duration transient increase in intensity that is maximum across a narrow frequency range [2]. In certain conditions, embolic signals appear to be markers of increased stroke risk and may be useful in patient management [3]. One of the problems in detecting emboli is the identification of an embolic signal caused by very small 'microemboli'. The intensity of the embolic signal may be so small as to require some sort of advanced processing techniques to distinguish these signals from Doppler signals arising from red blood cells.

The most familiar of methods employed by commercial Doppler ultrasonic systems are based on the fast Fourier transform (FFT). The result presented as sonogram, forms a time-frequency representation of Doppler signals obtained by first segmenting the data into frames and then

taking the FFT of each frame. Although the FT assumes that the signal is stationary, in practice, most natural signals, including Doppler signals are non-stationary. In order to characterize it properly, it is necessary to observe evolution of the signal both in time and frequency. The short time or windowed Fourier transform (WFT) has been used widely as it partially fulfils these requirements. It is given by

$$F_s(t, \nu) = \int_{-\infty}^{+\infty} s(\tau) g^*(\tau - t) e^{-j2\pi\nu\tau} d\tau \quad (1)$$

where $g(t)$ is a short time analysis window localized around time $t=0$ and frequency $\nu=0$. Because multiplication by relatively short window effectively suppresses the signal outside a neighborhood around analysis time point $\tau=t$, the WFT is a local spectrum of the signal $s(t)$ around a particular t . The frequency resolution of the WFT is proportional to the effective band-width of the analysis window. Consequently, for the WFT, there is a trade-off between time and frequency resolution: on one hand, a good time resolution requires a short window; on the other hand, a good frequency resolution requires a long window. Unfortunately, these conditions can not be simultaneously granted.

Using longer frame sizes may cause transient behavior of the blood flow to be missed. In this context, the wavelet transform (WT) may be used to study and understand the behavior of blood flow. In particular, it appears well-suited candidate to detection and analysis of transient embolic signals. The WT, which is increasingly applied in fields ranging from communications to medicine has a great potential for analyzing the signals with transient or nonstationary components [4,5]. By non-stationary, it is meant that the frequency content of the signal may change over time and the onset of changes in the signal cannot be predicted in advance. Embolic signals, which are reported to be transient-like and very short duration, fit the definition of non-stationary signals. Like the WFT based time-frequency representation, a complete WT process creates a two (or three) dimensional representation of a one-dimensional signal, typically with the horizontal axis

as time and vertical axis corresponding to the wavelet scale. The dimension is ‘number of samples×number of scales’. The third dimension (color in 2D display) is the amplitude of the WT coefficients. This representation allows exact localization of any abrupt change, or an exact time and duration of a short signal, which may not be evidenced by conventional signal processing techniques. The continuous wavelet transform (CWT) is performed by projecting a signal $s(t)$ onto a family of zero-mean functions (the wavelets) deduced from an elementary function $\Psi(t)$ (the mother wavelet) by translations and dilations. It is given by

$$W_s(a,b) = \frac{1}{\sqrt{|a|}} \int_{-\infty}^{+\infty} s(t) \psi^* \left(\frac{t-b}{a} \right) dt \quad (2)$$

where $*$ denotes the complex conjugate and $\psi^*(t)$ is the analyzing wavelet. The variable a (>0) controls the scale of the wavelet, such that taking $|a|>1$ dilates the wavelet ψ and taking $|a|<1$ compresses ψ . The variable b is the time translation and controls the position of the wavelet.

The wavelet transform is characterized by the following properties:

1. It is a linear transformation,
2. It is covariant under translations:

$$s(t) \rightarrow s(t-u) \quad W(a,b) \rightarrow W(a,b-u) \quad (3)$$

3. It is covariant under dilations:

$$s(t) \rightarrow s(kt) \quad W(a,b) \rightarrow k^{-1/2} W(ka, kb) \quad (4)$$

The basic difference between the CWT and the WFT is that when the scale factor a is changed, the duration and the bandwidth of the wavelet are both changed but its shape remains the same. The CWT uses short windows at high frequencies and long windows at low frequencies in contrast to the WFT, which uses a single analysis window. This partially overcomes the time resolution limitation of the WFT. The bandwidth B is proportional to the frequency ν . The CWT can also be assumed as a filter bank analysis composed of band-pass filters with constant relative bandwidth.

If $W(a,b)$ is the WT of a signal $s(t)$, then $s(t)$ can be restored using the formula:

$$s(t) = \frac{1}{C_\psi} \int_{-\infty}^{+\infty} \int_{-\infty}^{+\infty} W(a,b) \psi \left(\frac{t-b}{a} \right) \frac{da db}{a^2} \quad (5)$$

providing that the Fourier transform of wavelet $\psi(t)$, denoted $\Psi(\nu)$ satisfies the following admissibility

condition:

$$C_\psi = \int_{-\infty}^{+\infty} \frac{|\Psi(\nu)|^2}{\nu} d\nu < \infty, \quad (6)$$

which shows that $\psi(t)$ has to oscillate and decay. One of the original wavelet functions is the Morlet wavelet [6], which is obtained by taking a complex sine wave, and localising it with a Gaussian envelope and given by

$$\psi(t) = \pi^{-1/4} (\cos \omega_0 t + i \sin \omega_0 t) e^{-t^2/2} \quad (7)$$

where ω_0 is nondimensional frequency and usually taken to be 5 to 6 to satisfy the admissibility condition.

2. METHOD

50 consecutive embolic signals used for this study were recorded from patients with symptomatic carotid stenosis using a commercially available transcranial Doppler system (EME Pioneer TC4040) with a 2MHz transducer. For inclusion two experienced observers had to agree that the signal was an embolic signal using standard criteria [7]. Recordings were made from the middle cerebral artery using an axial sample volume of 5 mm. The time domain quadrature Doppler signal was saved to disk and imported to the PC. The sampling frequency of these signals was 7150 Hertz and the data length was 2048 point (286 ms). The data were prepared to include embolic signals at the first 143 ms part of the total recordings. The second 143 ms of the data were used to calculate average background Doppler ultrasound power.

The data were analysed using both the WFT and the CWT. The recorded quadrature signals were converted into directional format by applying the Hilbert transform process [8]. After obtaining directional Doppler signals, successive groups of 64 samples with a 99% overlap ratio (63 points) were taken and a data matrix having 64×2048 samples was created for subsequent 64 point FFT analysis. In order to include the last 63 sample points for FFT analysis, 63 zeros were added as necessary samples. 64 point FFT preceded by a 64 point Hanning window was applied. This process produces a 64×2048 point data matrix representing time-frequency distribution of a directional Doppler signal. For the CWT analysis, a 32 scale WT using Morlet wavelet was applied to both forward and reverse signals, producing a total of 64×2048 data array representing the time-scale distribution of the signals.

The time-frequency representation of embolic signals using the WFT and the CWT was compared by calculating embolic signal to background blood signal ratio (EBR),

half width maximum, and embolic signal onset (ESO). The time-frequency distribution was integrated over all frequencies/scales to give an estimate of the instantaneous power of the signal [9]. The half width maximum for the time resolution (HWMT) was defined as the temporal distance between the point at which power reached half maximum and the point at which it fell to half maximum. This is an indication of the variability of temporal resolution as a function of a certain transform parameter considered. The time-frequency distribution integrated over all time should approximate the energy spectrum of the signal [9]. The half width maximum for frequency resolution (HWMF) was defined as the distance between the two 50% powers of the normalised energy spectrum. This parameter indicates the amount of the frequency spread depending on the transform parameter considered. The accuracy with which each method described the position of an embolic signal in time was estimated by measurement of the ESO, which was measured at two tenth of the maximum instantaneous power. The ESO indicates how the time localisation properties of the transforms are influenced by the transform parameters considered. These were compared with the ESO values estimated from the directional time domain signal. This was taken as reference and the ESO values for the WFT and CWT were found. The EBR was defined as

$$EBR = 10 \log \frac{A_{peak}}{B_{avg}} \quad (8)$$

where A_{peak} is the power at frequency (scale for the WT) with maximum intensity during the first half of the data record, and B_{avg} is the average power of the background intensity. The latter was calculated by time and frequency/scale averaging of the time-frequency analysis results [10] using the second half of the total data.

3. RESULTS

Mean and standard deviations of the EBR, HWMF, HWMT and ESO for the 50 embolic signals are presented in Table 1. The mean EBR for the CWT and the WFT was almost the same. The HWMT for the CWT was better than that of the WFT. The HWMF for the CWT was also better than the WFT. In fact, the HWMT and HWMF for the WFT are a function of the window size. Longer window sizes result in an increased frequency resolution, hence better HWMF, shorter window sizes result in an increased time resolution, hence better HWMT. In contrast, the CWT results in an optimized HWMT and HWMF values. Time localisation using the CWT was also much better than the WFT and shows very close agreement with the measurement from the time domain signal.

	EBR(dB)	HWMT(ms)	HWMF(Hz)	ESO(ms)
WFT	15.31(2.62)	11.24(9.91)	664(377)	66.56(7.7)
CWT	15.35(2.38)	10.21(9.34)	350(339)	67.29(7.67)
ESO measured from time domain signals (ESOT)				
				67.85(7.64)
2-tail Probability				
CWT vs WFT	0.8335	<0.0001	<0.0001	0.0002
ESOT vs WFT				<0.0001
ESOT vs CWT				0.0077

Table 1. Mean (and standard deviations) of the EBR, HWMT, HWMF, and ESO for the 50 embolic signals, and 2-tail probability values.

4. CONCLUSION

Since it has a direct effect on the WFT results, the analysis window size is the most influential parameter. The time resolution is better and frequency resolution is poorer for shorter windows, the time resolution is poorer and the frequency resolution is better for longer windows. 64 point window size reasonably reflects the time-frequency behaviour of embolic signals as shown in Figure 1.

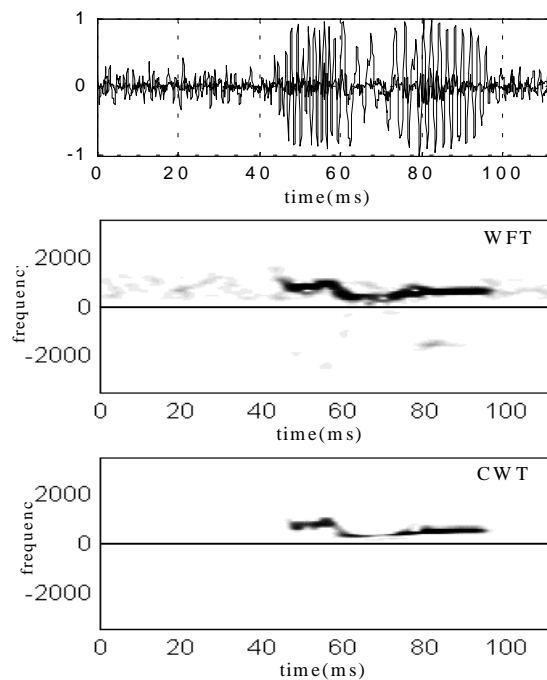


Figure 1. Time-frequency distributions of an embolic signal with the WFT (64 point Hanning window) and the CWT (32 scales Morlet wavelet).

Here, the signal has two humps and a complex frequency structure. As the wavelet transform is local both in time and frequency domains, the time-frequency representation of an embolic signal using the WT is optimized in terms of the time-frequency resolution. This is apparent from the Figures 1 and 2, where the CWT results appear to be clearer confirming the results presented in Table 1.

The wavelet transform appears well suited to the analysis of embolic signals offering an optimised time-frequency resolution and superior time localisation compared to the WFT as evidenced in Table 1 and illustrated in Fig. 3. This is because of the unique property of the wavelet transform, which is important for the detection and analysis of nonstationary and fast transient signals such as embolic signals. When the scale is small the wavelet is concentrated in time and the wavelet analysis has a detailed view of the signal. When the scale increases the wavelet spreads out in time and the wavelet analysis has a global view of the signal. As a result, the CWT increased embolic signal conspicuity assessed visually, compared with the WFT as demonstrated in Fig. 2. Consistent with the visual assessment, the CWT has an optimized temporal resolution and the best EBR as given in Table. 1.

Since the results obtained by the CWT heavily depend upon the choice of an appropriate wavelet, constructing a better wavelet will more accurately describe embolic signals and result in higher amplitude wavelet coefficients, and hence a higher EBR value. The results obtained with a standard wavelet suggests that the wavelet transform is well suited to detect and analyse short duration embolic signals. It is also possible that a real-time embolic signal detection and analysis system based on the fast wavelet transform can be implemented.

5. REFERENCES

- [1] MP Spencer, GI Thomas, SC Nicholls, LR Sauvage. "Detection of middle cerebral emboli during carotid endarterectomy using transcranial Doppler ultrasonography". *Stroke*, 21:415-423, 1990.
- [2] HS Markus, C Tegeler. "Experimental aspects of high-intensity transient signals in detection of emboli". *J Clin Ultrasound*, 23:81-87, 1995.
- [3] HS Markus, MJ Harrison. "Microembolic signal detection using ultrasound". *Stroke* 26:1517-9, 1995.
- [4] M Akay. "Wavelets in biomedical engineering". *Annals of biomedical Engineering*, 23:531-542, 1995.
- [5] O Rioul, M Vetterli. "Wavelets and signal processing". *IEEE Signal Proc Magazine*, 8:14-38, 1991.
- [6] RK Martinet, J Morlet, A Grossmann. "Analysis of sound patterns through wavelet transforms". *International J of Pattern Recogn and Artificial Intellig*, 1:273-302, 1986.
- [7] EB Ringlestein, DW Droste, VL Babikian, DH Evans, DG Grosset, M Kaps, HS Markus, D Russell, M Siebler. "International Consensus Group on Microembolus Detection. Consensus on microembolus detection by TCD". *Stroke*, 29:725-729, 1998.
- [8] N Aydin, L Fan, DH Evans. "Quadrature-to-directional format conversion of Doppler signals using digital methods". *Physiol Meas*, 15:181-199, 1994.
- [9] WJ Williams, T Sang, JC O'Neill, EJ Zalubas. "Wavelet windowed time-frequency distribution decompositions". *SPIE*, 3162:149-160, 1997.
- [10] C Torrence, GP Compo. "A practical guide to wavelet analysis". *Bull Amer Meteor Soc*, 79:61-78, 1998.

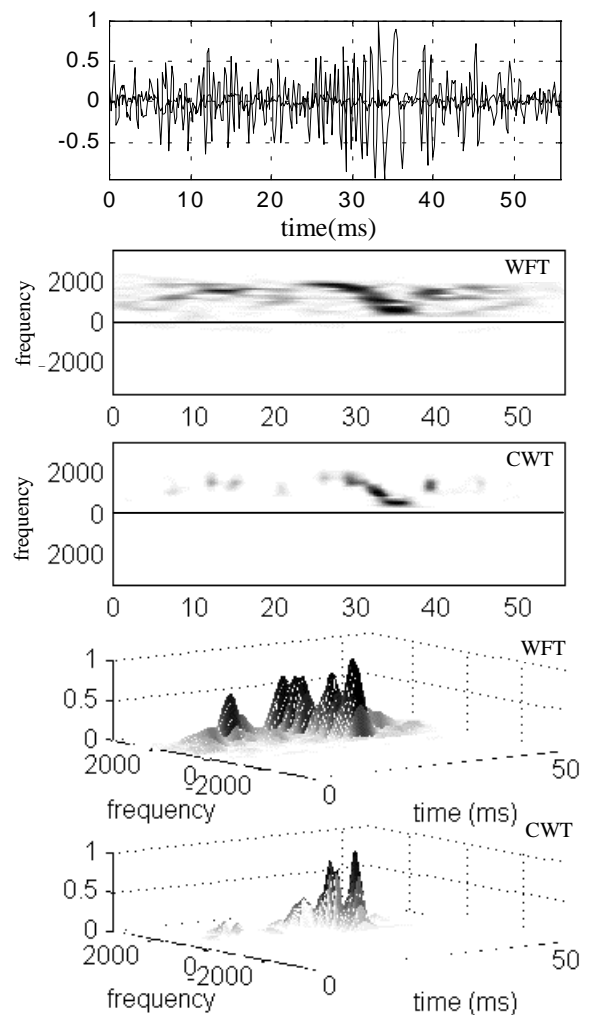


Figure 2. A low intensity embolic signal including forward and reverse flow components and corresponding two and three dimensional intensity plots of the WFT (64 point Hanning window) and the CWT (32 scales Morlet wavelet) results (- indicates reverse flow direction).

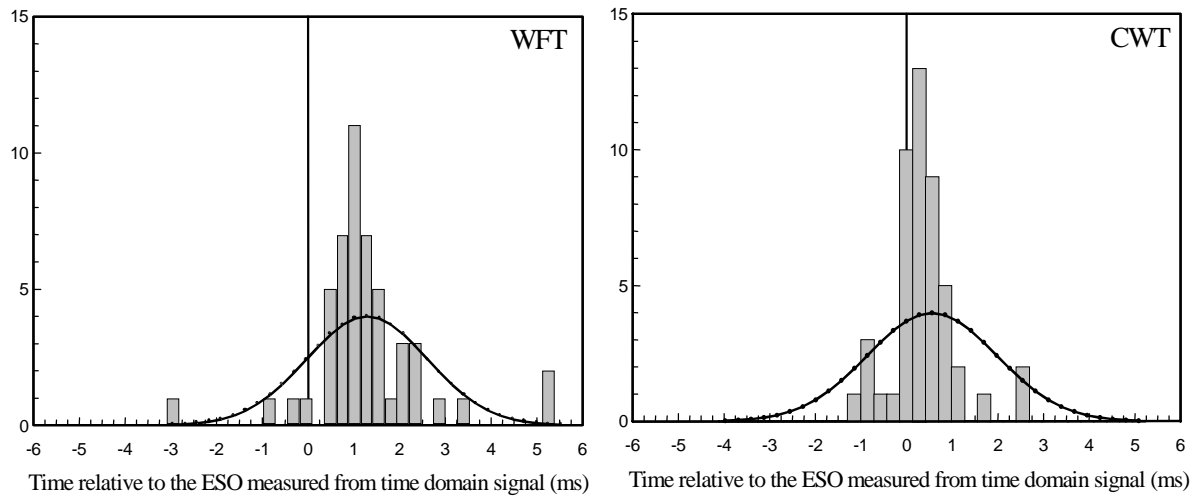


Figure 3. Histograms illustrating the distributions of time localisation estimates for the CWT and the 64 point WFT (after compensation for the time shift introduced by 99% overlapping used for FFT).